Transactions, SMiRT-25
Charlotte, NC, USA, August 4-9, 2019
Division V

FE ANALYSIS OF REINFORCED CONCRETE STRUCTURES UNDER MISSILE IMPACT USING SUB-MODELLING TECHNIQUE

Genadijs Sagals[1], Nebojsa Orbovic[1], and Thambiayah Nitheanandan[2]

[1] Technical Specialist, Canadian Nuclear Safety Commission, Ottawa, Ontario, Canada
[2] Director, Canadian Nuclear Safety Commission, Ottawa, Ontario, Canada

ABSTRACT

This paper describes the work conducted by the Canadian Nuclear Safety Commission (CNSC) related to the numerical simulations of reinforced concrete (RC) structures under deformable missile impact. The current paper is a continuation of the work conducted in the frame of the OECD/NEA[4] IRIS (**I**mproving **R**obustness Assessment Methodologies for Structures **I**mpacted by Missile**s)** Phase 3 benchmark project.

The concrete mock-up with two simple structures attached, one welded and another bolted, was built and tested at the VTT Technical Research Centre in Espoo, Finland. This mock-up was impacted by three subsequent missiles with varying velocities in order to obtain the damage accumulation. To examine vibration transmission through the mock-up, the simple structures modelling equipment were attached to the rear wall of the structure, while the missile impact was at the centre of the front wall. The parameters of the missiles and the RC structure were selected to ensure a flexible behaviour of the RC target in the impact area with only moderate damages, specifically cracking and permanent deformation without perforation.

Detailed modelling of a large RC structure with all equipment attached leads to a very large finite element (FE) model. Therefore, a two-level FE modeling using a commonly used sub-modelling approach was employed: first, analyze the vibrations of a reinforced concrete structure with simplified equipment modelling, and second, analyze in detail the equipment connected to it. This approach assumes uncoupled dynamic behaviour of the structure and the equipment.

The non-linear dynamic behaviour of the reinforced concrete slabs under missile impact was analyzed using the commercial FE code LS-DYNA. Both 3-D solid and 2-D shell FE models were employed for the target discretization. Since the ultimate objective of this work is to model the entire structure over long time periods, a simplified combined shell-solid model with distributed (smeared) reinforcement was selected and validated. This model employs solid FE around an impact area and shell FE for the rest of the mock-up.

"Blind" (without knowing test results) FE predictions were compared to tests conducted at the VTT test facility. As a result, the FE model was revised to better match the test data. The revised model shows good agreement with the test results for both global (RC mock-up) and local (equipment) behaviour. To select adequate damping and cut boundaries for sub-models sensitivity analysis was conducted.

1. INTRODUCTION

Modern Canadian and International design codes and regulatory documents for Nuclear Power Plants require design against impact of externally or internally generated missiles on safety related concrete structures. This requirement stimulated a large amount of analytical and experimental work conducted in

different countries. The most noticeable tests were conducted in Germany (so called Meppen Impact Tests, Nachtsheim and Stangenberg (1981)), the full scale test at Sandia (Sugano et al. (1993)) and in Finland (Impact I-III tests conducted by VTT Technical Research Centre, Vepsä et al. (2011)). Based on publicly available data from these tests, two simulation workshops IRIS_2010 and IRIS_2012 were conducted (Vepsä et al. (2011), Berthaud et al. (2011) and Orbovic et al. (2015)). The authors of the current paper actively participated in both workshops and developed an adequate FE model (Sagals et al. (2011) and Orbovic et al. (2015)) that is capable of predicting the main characteristics of post-impact state of a concrete slab, such as perforation velocity, size and shape of damaged area, crack patterns, etc.

The impact-induced vibrations were, however, not addressed in previous studies. No tests have been conducted to examine impact induced vibrations and their propagation through a reinforced concrete structure. Therefore, it was decided to conduct the new international simulation workshop IRIS Phase 3 in the framework of the OECD/NEA, with the main objective to analyze the transmission of the impact induced vibrations through a reinforced concrete structure from the impacted wall to the floors and walls of the structure which are outside the impacted area. The description of the experimental set-up and preliminary analysis of the mock-up are provided in Vepsä et al. (2016), Hervé (2017) and Borgerhoff et al. (2017).

The IRIS 3 benchmark was not completed at the time of writing this paper. Therefore, only partial results for the mock-up shown in Figure 1 are presented in the current paper. The main objective was to verify the selection of sub-model and compare FE predictions with test results for some output parameters.

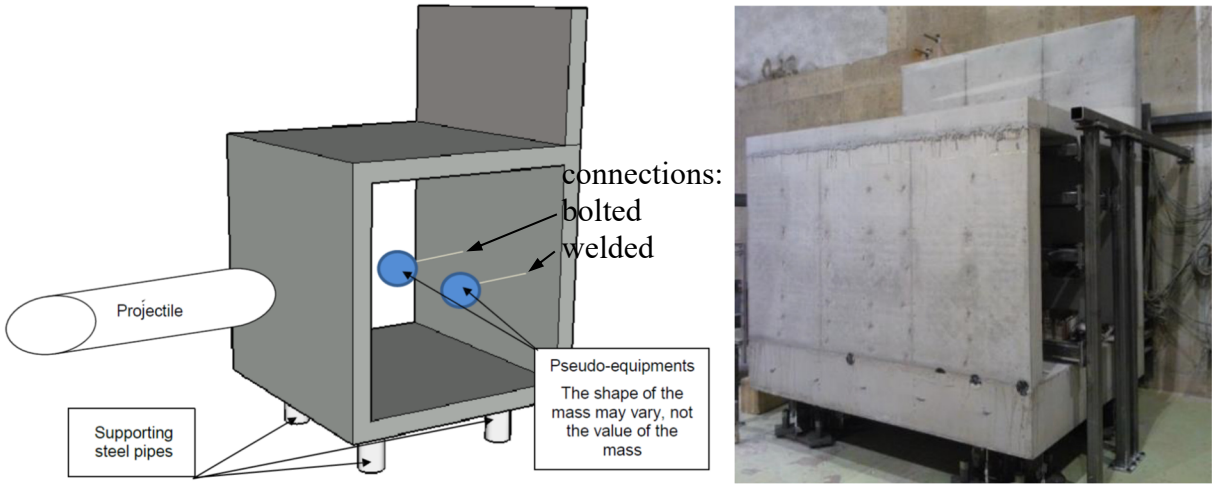

Figure 1. Concrete mock-up.

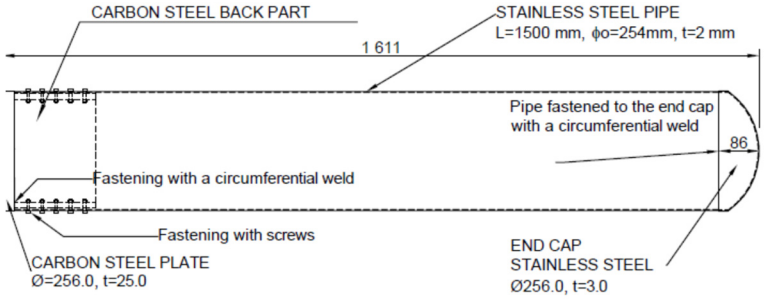

Test #	Velocity m/s	Length m	Mass kg
1	91.8	1.611	50.1
2	93.5	1.611	50.1
3	167.0	2.511	50.26

Figure 2. Missiles used in tests.

2. FE MODELING

As mentioned in the previous section, the authors have an existing FE model that was successfully used for modelling the missile impact on the reinforced concrete slab. This model is based on the commercial explicit code LS-DYNA (LS-DYNA® R8.0 (2015)). However, this model includes fine 3-D mesh with solid FE and explicit modelling of reinforcement. Using this type of FE model for a structure consisting of several slabs with an extended simulation time to capture the impact induced vibrations leads to long modeling times. Additionally, authors believe that this approach is impractical for larger structures, such as a nuclear containment building.

The test runs conducted show that a simplified all-shell model of the mock-up, however, does not produce adequate results as described in section 3.1 below. Therefore, a new simplified hybrid model was developed to simulate mock-up behavior. This model consists of solid FE around the impact zone and shell FE for the rest of the mock-up and the missile. The detailed description of this new model is provided below.

2.1 FE Model of the concrete mock-up

Figure 3 shows the new hybrid solid/shell model developed for the second mock-up. It was assumed that attached pseudo-equipment will not significantly influence the mock-up behavior. In this case, only one half of the entire model with simplified welded "equipment" could be analyzed first.

The following additional assumptions were made:

- Detailed models of both welded and bolted "equipment" were analyzed separately after obtaining the entire system behavior (sub-modeling technique). The selection of these sub-models is described below in section 3.2.
- Hybrid shell/solid FE mesh with solid FE around the impact area of the front wall and shell FE for the missile and the remaining part of the mock-up were selected
- Each attached leg was modeled as a set of equivalent springs connected to the mock-up floor and ground.

  Loading sequence:
- 3 missiles were defined for subsequent impacts with impact velocities 91.8, 93.5 and 167 m/s (as in tests)
- 1000 ms simulation time was selected for each impact with additional 200 ms between impacts for relaxation of induced vibrations before the next impact

2-D Belytschko-Tsay 4-noded shell FE was used for mock-up and missile modeling, except the front wall around the impact area. 3-D solid 8-noded FE with constant stress was used in this area. The connection between solid and shell FE was modeled using command CONSTRAINED_SHELL_TO_SOLID that aligns brick nodes lying along the tangent vector to the nodal fiber, see Figure 3. Simplified pseudo-equipment (welded) was modeled using four 3-D Belytschko-Schwer resultant beams and rigid cylinder.

2.2 Detailed modeling of pseudo-equipment

Figure 4 shows the attached pseudo-equipment. During the analysis of the half of the entire model all nodal displacements at the selected sub-model interface were saved for the subsequent detailed modeling of the pseudo-equipment using LS-DYNA command *INTERFACE_LINKING_ NODE_SET. After finishing the analysis, saved interface displacements were applied as BC to interface nodes for the newly developed detailed sub-models for both welded and bolted pseudo-equipment as shown in Figure 5. Separate runs were conducted for each sub-model.

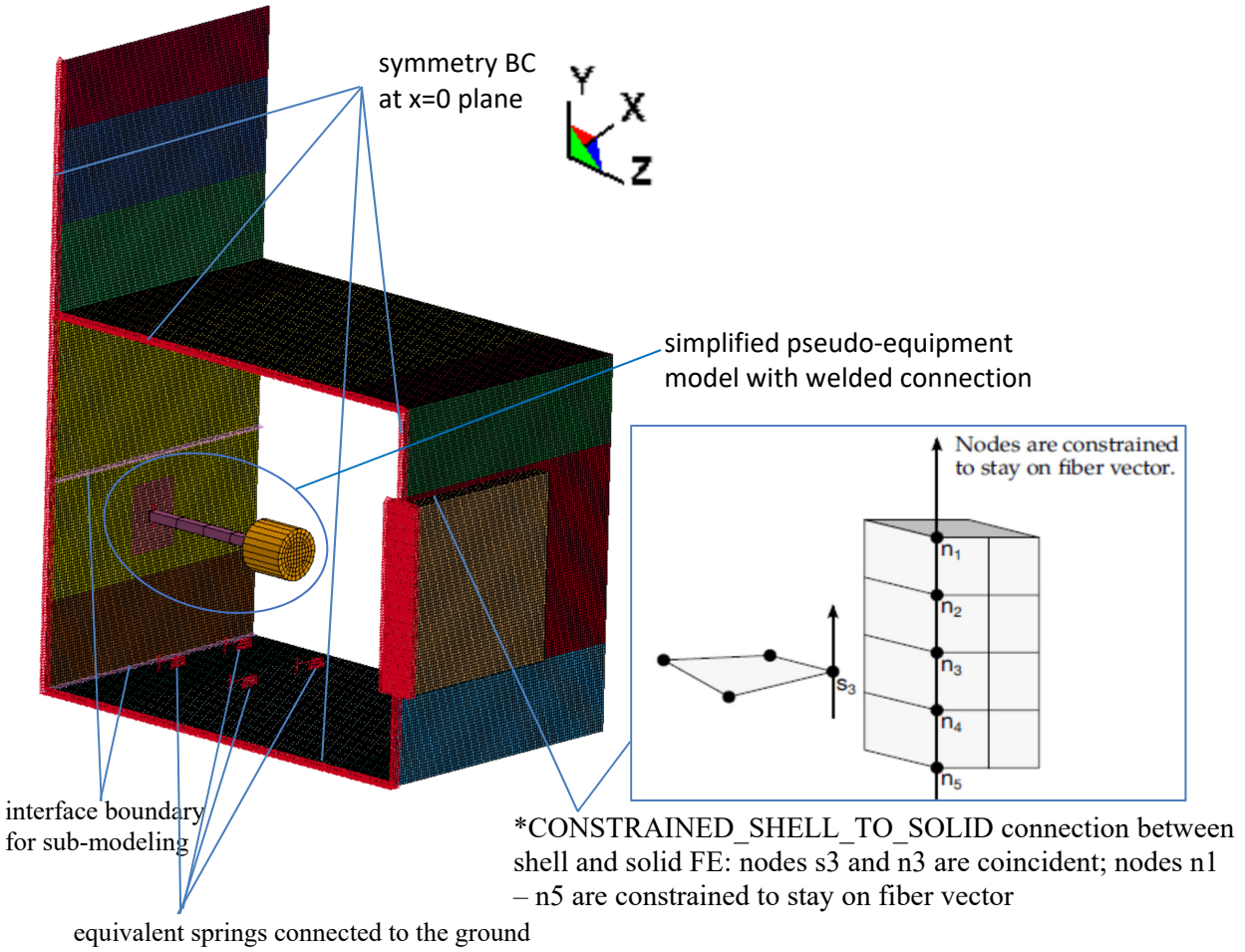

Figure 3. ½ of the entire mock-up model with selected interface boundaries and simplified welded pseudo-equipment.

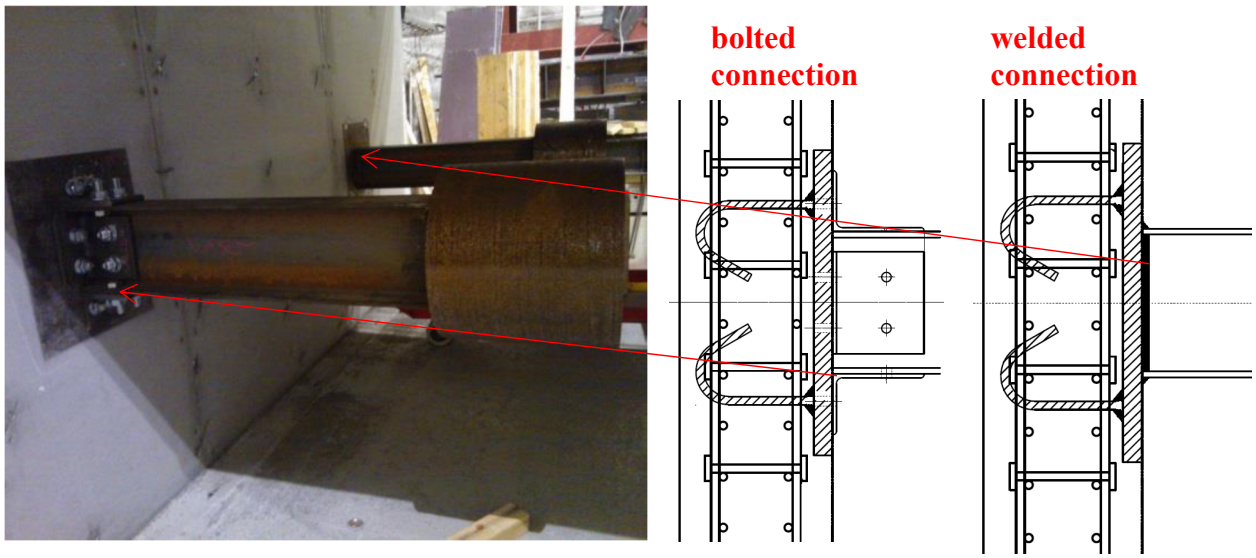

Figure 4. Pseudo-equipment attached to the rear mock-up wall.

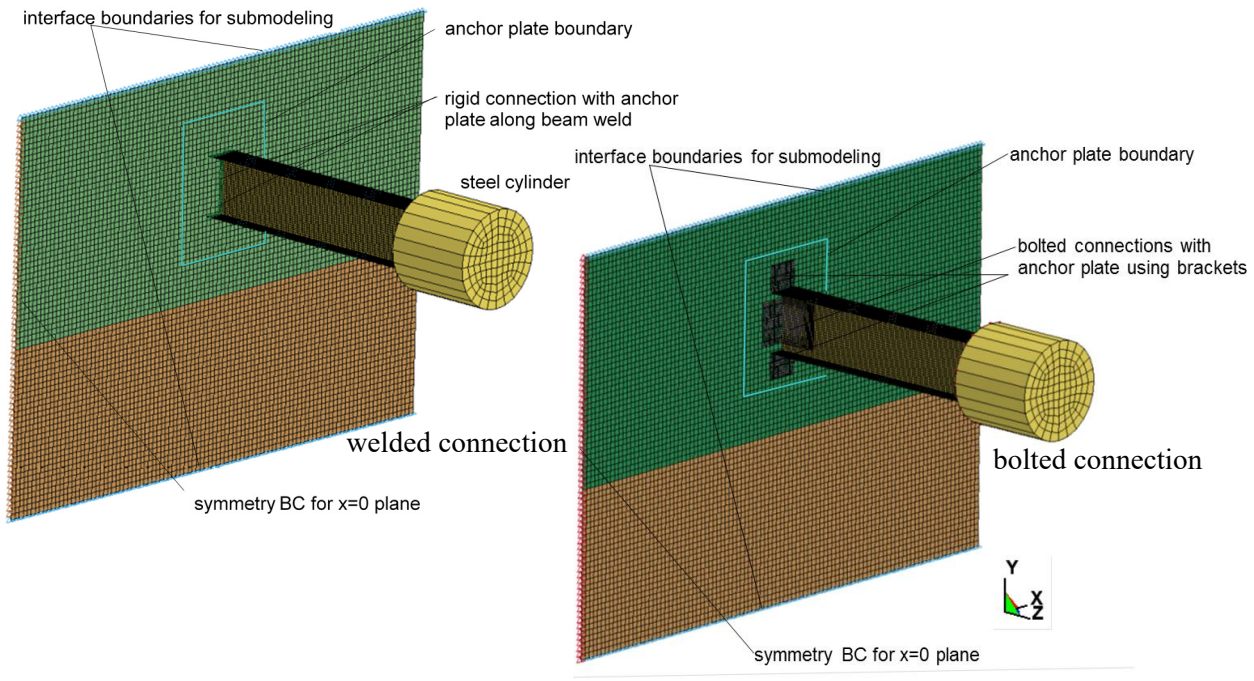

Figure 5. Detailed models of attached pseudo-equipment

2.3 Material models and parameters

Material parameters were selected as measured in tests. The following material models were selected for analysis:

Steel Missile:

2-D Belytschko-Tsay 4-noded shell FE with bilinear plastic-kinematic material (MAT_003 in LS-DYNA) E=200GPa, ν=0.3, σ_y=344MPa, σ_u=616MPa, E_t=573MPa, fracture strain 47.4%, Cowper-Symonds strain-rate model was selected: C=100 1/s, p=10

Concrete Mock-up:

3-D (solid) part (front wall around the hit point) was modeled using *MAT_WINFRITH_ CONCRETE without strain-rate:

E=28.86GPa, ρ=2500kg/m^3, ν=0.17, UCS= 59.4MPa (cubic), UTS= 2.88MPa, aggregate size=8mm (Ø), default pressure versus volumetric strain curve.

Reinforcement for solid FE:

Smeared (distributed) reinforcement with identical material properties in x-, y- and z-directions was selected. Fraction of reinforcement in each direction was calculated as ratio of reinforcement to concrete areas in that direction:

E=200GPa, σ_y=524MPa (Ø6mm wall reinforcement), Et=708MPa, ultimate elongation=20.57%.

Concrete 2-D parts were modeled using *MAT_CONCRETE_EC2 (Material data and equations governing the behavior are taken from Eurocode 2 Part 1.2 (General rules – Structural fire design), hereafter referred to as EC2):

Front and back walls:

ρ=2500kg/m^3, UCS= 52MPa (cylinder), UTS= 2.88MPa

Cantilever wall:

ρ=2500kg/m^3, UCS= 47MPa (cylinder), UTS=2.3 MPa

Floor:

ρ=2500kg/m^3, UCS= 52.6MPa (cylinder), UTS= 2.92MPa

Top horizontal wall:
ρ=2500kg/m^3, UCS= 62.4MPa (cylinder), UTS= 2.42MPa

Reinforcement for shell FE:

Smeared (distributed) reinforcement was selected for both 3-D and 3-D FE. Transverse reinforcement is not allowed for shell FE used. Fraction of reinforcement in each direction was calculated as ratio of reinforcement to concrete areas in that direction:
E=200GPa, ν=0.3, σ_u=666.3MPa (Ø6mm floor reinforcement), 614.7MPa (Ø10mm floor reinforcement), 670MPa (Ø6mm wall reinforcement), other parameters- default values for selected reinforcement model.

Pseudo-Equipment:

S355 steel for both beams and anchor plate:
E=200GPa, ν=0.3, σ_y=355MPa, σ_u=550MPa
Rigid material was selected for steel cylinder

Default values were selected for other remaining reinforcement and concrete parameters according to FE models requirements.

2.4 Damping

Rayleigh damping C=α*M+β*K was applied to concrete parts as follows:

1. During the impact phase α=4.66 1/s for 2-D shells (~1% of critical damping), α=11.64 1/s for 3-D solids (~2.6% of critical damping), β=0.005 s. Critical damping was defined using the 1st calculated bending frequency of back and top walls 35.37Hz.
2. During the relaxation stage α=93.0 1/s (~20% of critical damping), β=0.005 s for all concrete FE. Increased damping was selected to suppress residual post-impact oscillations and get a steady-state of the mock-up before the next impact.

For pseudo-equipment Rayleigh damping was applied as follows:

1. During the impact phase α=1.14 1/s (~0.5% of critical damping), β=0. Critical damping was defined using the 1st calculated bending frequency of welded pseudo-equipment 17.41Hz.
2. During the relaxation stage α=228.0 1/s (~100% of critical damping), β=0.

2.5 Boundary conditions modeling

Four sets of springs with one end attached to the mock-up floor and the other end attached to the ground were used to model each leg, see Figure 3. Each set consists of 3 elastic springs in x-, y- and z-directions. The stiffness of each spring was selected to ensure the same leg displacements under static loads along these axes. Additionally, symmetry boundary conditions (BC) were applied at plane x=0 to adequately model ½ of the entire model.

3. MODELING RESULTS

Modeling results were arranged into three groups as follows: (i) comparison between different FE models to establish adequate model and mesh density, (ii) selection of the appropriate sub-model, and (iii) comparison of FE predictions for selected output variables with test results.

3.1 Comparison between different FE models

As was mentioned earlier in Section 2, the use of a detailed 3-D solid FE for the entire mock-up is impractical. However, the fully 3-D solid and fully shell models were created and compared to ensure that a shell model could adequately transfer impact induced vibrations from the impact zone to the rest of the system and, specifically, to the back wall. Mesh convergence study was also preformed to select adequate mesh size. The modelling results (Sagals et al. (2017)) show that:

- The hybrid mock-up model produced better results (closer to test results) compared with the fully shell model, particularly in the impact zone, and

- A mesh size of approximately 10 mm (approximately 200 FE across the entire mock-up width in the x-direction and, additionally, 8 FE through the thickness for the solid part of the model) is adequate for modeling mock-up behavior. For the deformable steel missile, a mesh size of approximately 4.5 mm for the missile head and the part of the side shell close to the head and 11 mm for the remainder of the missile was determined to be adequate. Missile deformations and force transfer to the mock-up during impact and rebound were considered.

3.2 Selection of the appropriate sub-model

Sensitivity analysis was conducted to select an adequate sub-model that was used for detailed analysis of pseudo-equipment. Three different sub-models: "small", "medium" and "large" were selected during the first analysis of the one half of the entire model, see Figure 3. All these sub-models have the same simplified model of welded pseudo-equipment. The difference is in the included area of the back wall as follows:

- 250mm×350mm area of the back wall is included in the "small" sub-model. This area includes only pseudo-equipment anchor plate and underlying concrete wall,
- 350mm×450mm area of the back wall is included in the "medium" sub-model. This area includes also strips of concrete wall around pseudo-equipment anchor plate, and
- 1250mm×888mm area of the back wall is included in the "large" sub-model. This area covers the entire width of the ½ of back wall.

As described in section 2.2, all nodal displacements at the selected sub-model interfaces were saved for the subsequent detailed modeling of the pseudo-equipment using LS-DYNA command *INTERFACE_LINKING_NODE_SET. After finishing the first stage, saved interface displacements were applied as BC to interface nodes for the detailed sub-models for both welded and bolted pseudo-equipment. Identical detailed models of pseudo-equipment were used for the second stage. The only difference was in the size of the back wall around pseudo-equipment anchor. Separate runs were conducted for each sub-model of welded or bolted pseudo-equipment. To decrease modeling time, only 200 ms were modeled for each impact following by 200 ms of relaxation. Therefore, the total modeling time was 1200 ms instead of 3600 ms used in the next section for comparison with test results.

Figure 6 shows vertical (y) and horizontal (x and z) displacements at the center of steel cylinder for all selected sub-models. The results clearly show "abnormal" behavior of horizontal displacements of the "small" sub-model during the third impact. Both "medium" and "large" sub-models show similar behavior during the all three impacts with some small differences between them. FE predictions for these sub-models are similar to the predictions for the entire model. Therefore, the "large" sub-model was selected for both welded and bolted pseudo-equipment.

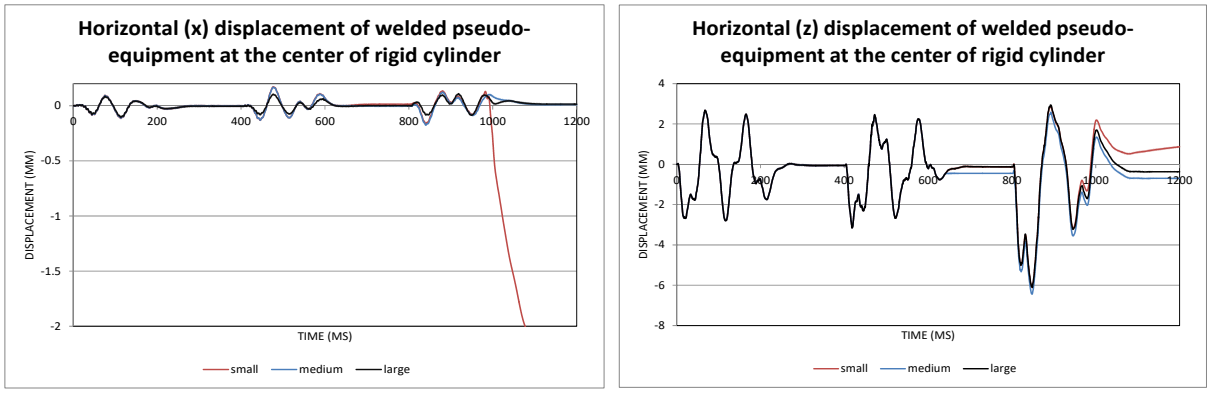

Figure 6. Displacements at the center of steel cylinder for all selected sub-models.

3.3 Mock-up results

With respect to the mock-up, the global damage, displacements, accelerations and support forces were calculated and compared with the test results where possible. Of all test results for mock-up, the recorded displacements proved to be the most reliable. Therefore, in the current paper, the focus will be on mock-up displacements only. Figure 7 shows predicted and test displacements in z-direction during the first and third impact at two selected sensor locations: D01 and D7. These locations correspond to the beginning and the end of vibration propagation path. For the first impact the results show good agreement for the first peak for both locations. The main frequency of the post-impact vibrations is also well captured. However, test displacements decay more rapidly than in FE analysis and have larger permanent (residual) values.

During the second impact the selected displacements at sensor locations D01 and D7 were observed to be similar to the first impact with slightly higher amplitudes. Similar to the previous impacts, the results for the third impact show good agreement for the first maximum values for both locations. The main frequency of the post-impact vibrations was also well captured. Good agreement between FE predictions and test results was also obtained for displacements decay. Similar to previous two impacts, the residual values were larger for test results. However, the difference between predicted and test residual values (1.9% for bolted and 21.4% for welded connection) was significantly less for the third test, comparing with two previous tests.

The total concrete damping is the sum of applied Rayleigh damping and additional concrete damping implicitly employed in Winfrith and EC2 concrete material models. Sensitivity analysis conducted shows that damping optimization will not significantly improve model behavior. Probably, the real system damping evidenced in tests cannot be adequately modeled in available LS-DYNA material models. One of the possible reasons for a discrepancy in residual values could be the established fact that Winfrith model does not adequately predict concrete relaxation after impact (Orbovic et al. (2015)).

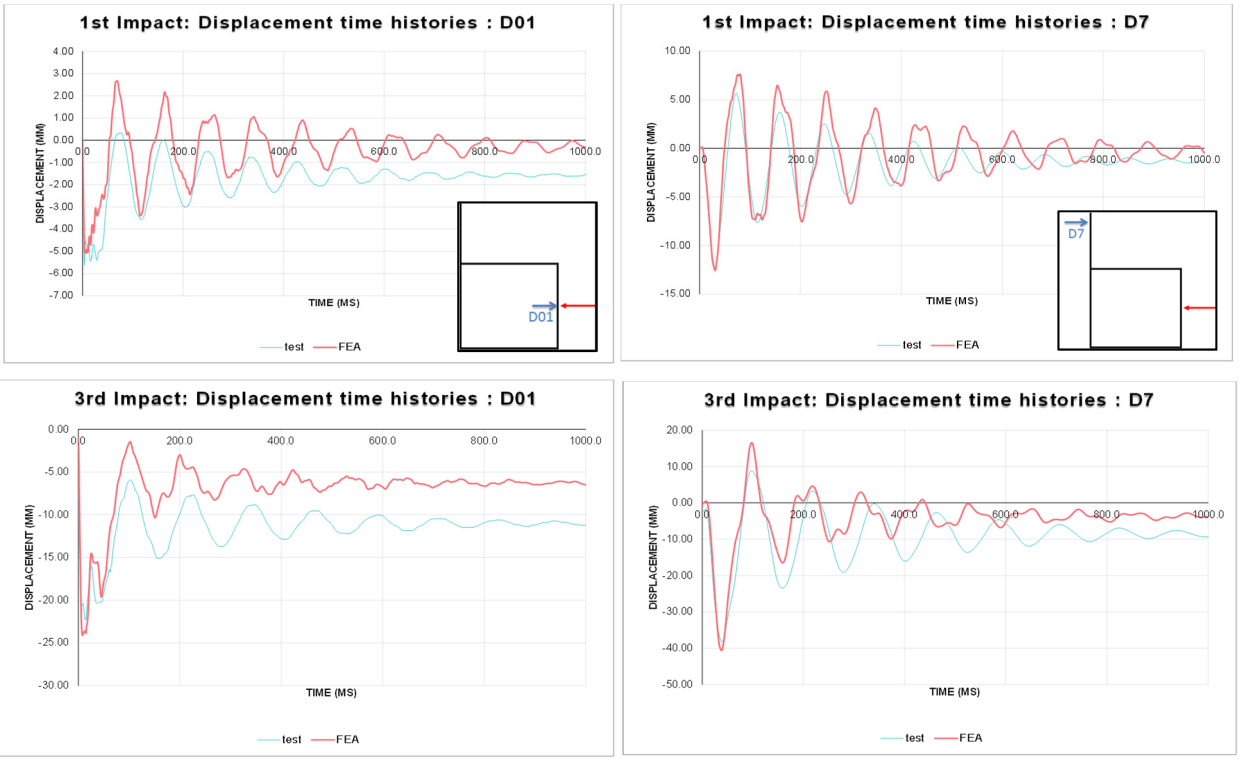

Figure 7. Displacements at sensors D01(z) and D7(z) during the first and third impacts.

3.4 Pseudo-equipment results

Figures 8 shows predicted and test displacements D10w (welded) and D10b (bolted) after the first impact at sensor locations. These displacements were calculated using both the full model (with simplified welded pseudo-equipment) and detailed sub-models. As expected, bolted connection leads to increased vertical displacements. No significant difference was observed between predictions for the simplified and detailed models of welded pseudo-equipment. Good agreement with test results was obtained for the main frequency of the impact-induced vibrations. However, the predicted maximum displacement at the first peak was 1.85 times less than test result for welded and 1.63 times less for bolted connection. The residual values of selected displacements were also higher for test results for both welded and bolted connections. However, the vibrations decay was similar for FEA predictions and test results. The main reasons for this discrepancy are, probably, the limitations of the shell model used for mock-up and inadequacy of Rayleigh and concrete material damping used in modeling. FEA predicted fully elastic pseudo-equipment behavior for welded connection. A very limited residual plasticity (ε_{pl}^{max}=0.4%) was predicted for bolted connection at the I-beam - anchor connection. Pseudo-equipment displacements for the second missile impact are similar to the displacements for the first impact with slightly higher amplitudes.

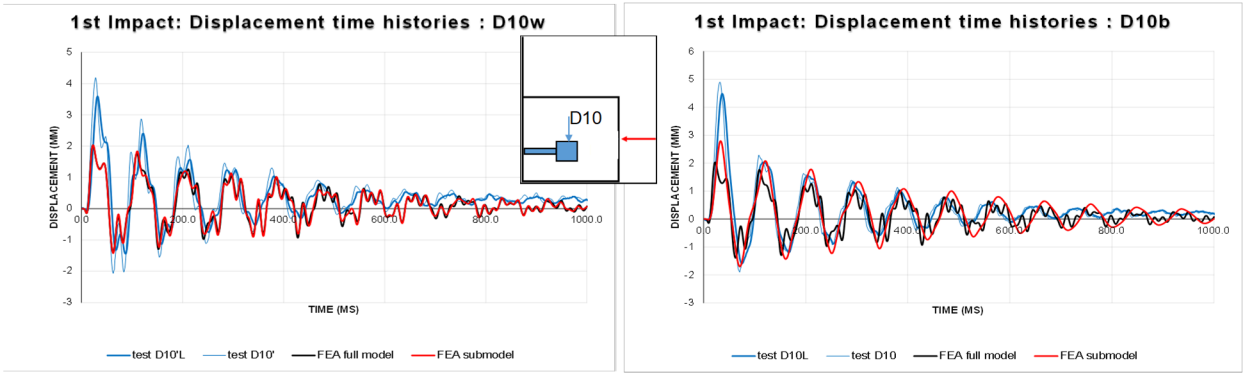

Figure 8. Displacements D10w (welded) and D10b (bolted) in y-direction during the first impact.

Finally, Figure 9 shows predicted and test displacements D10w (welded) and D10b (bolted) at sensor locations during the last (third) impact. As expected, bolted connection again leads to increased vertical displacements. Larger difference was observed between predictions for the simplified and detailed models of welded pseudo-equipment. FE predictions using the detailed model are generally closer to test results. The agreement with test results for the main frequency is not as good as for the previous two impacts. The difference between the predicted and test values of maximum displacements (the first peak) was less for the third impact comparing with the first two impacts: 1.15 times for welded and 1.25 times for bolted connection. The reasons for this discrepancy are the same as stated previously for the previous

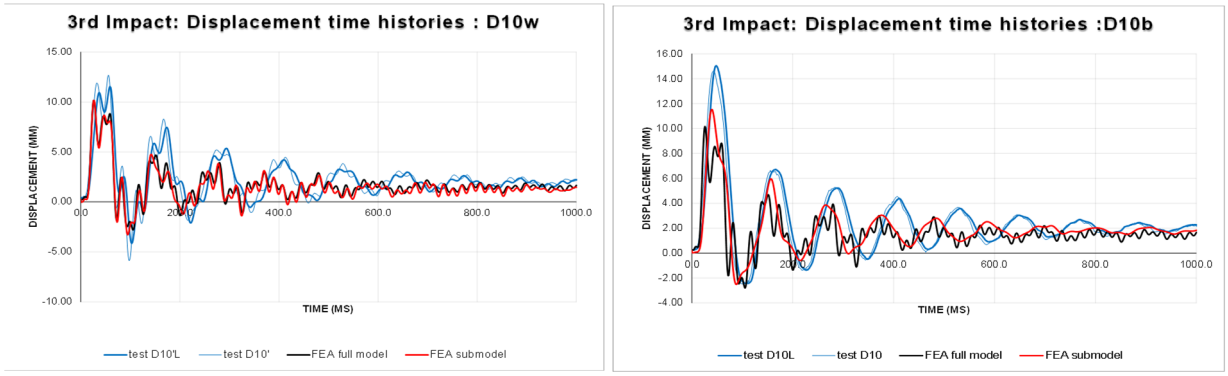

Figure 9. Displacement D10w (welded) and D10b (bolted) in y-direction during the last (third) impact.

two impacts. The residual values of selected displacements are also much closer for test results and FE predictions for both welded and bolted connections. Similar to previous two impacts, FEA predicted no residual plasticity for welded and significant residual plasticity (ε_{pl}^{max}=5.76%) for bolted connection.

CONCLUSIONS

The FE model developed using LS-DYNA provided a generally good agreement with test results for the mock-up deformations. Comparison with test results resulted in the following conclusions:

Mock-up

- Predicted maximum displacements at most sensor locations are in good agreement with test results for all three impacts.
- The main frequency of the post-impact vibrations is also well captured.
- Measured displacement decays are higher for the first two impacts and similar for the last (third) impact.
- Measured residual values are higher for all impacts. The difference is the smallest for the last impact.

Pseudo-equipment

- The difference between simplified and detailed models is insignificant for the first two impacts and much larger for the last impact.
- Bolted connection resulted in higher displacements.
- The difference in maximum displacements (first peak) is the largest for the first impact. For the last impact FEA predicts similar to test displacements for both welded and bolted connections

REFERENCES

Berthaud Y., Benboudjema F., Colliat J.-B., Tarallo F., Orbovic N., Rambach J.-M. (2011). "IRIS_2010 - Part IV: Numerical Simulations of Flexural VTT-IRSN Tests," *Transactions of the SMiRT 21*, New Delhi, India, pp 855-862.

Borgerhoff M., Stadler M., van Exel C., Schneeberger C., Stangenberg F., and Zinn R. (2017). "Induced Vibrations of a Reinforced Concrete Structure Tested in IRIS Phase 3 Project Subjected to Impact by a Deformable Missile," *Transactions of the SMiRT* 24, Busan, Korea.

Hervé, G. (2017). "Description of IRIS Phase 3 Project", in OECD-NEA, "Improving Robustness Assessment of Structures Impacted by a large missile at medium velocity **(**IRIS phase 3)".

LS-DYNA® R8.0 User's Manual, Livermore Software Technology Corp. (2015).

Nachtsheim W., Stangenberg F. (1981). "Impact of deformable missiles on reinforced concrete plates-comparisonal calculations of Meppen tests," *Transactions of the 6th SMiRT*, Paris, France.

Orbovic N., Tarallo F., Rambach J.-M., Sagals G. and Blahoianu A. (2015). "IRIS_2012 OECD/NEA/ CSNI benchmark: Numerical simulations of structural impact," *Nucl. Eng. and Design*, 295:700–715.

Orbovic N., Sagals G. and Blahoianu A. (2015). "Influence of transverse reinforcement on perforation resistance of reinforced concrete slabs under hard missile impact," *Nucl. Eng. and Design*, 295:716–729.

Sagals G., Orbovic N. and Blahoianu A. (2011). "Sensitivity Studies of Reinforced Concrete Slabs under Impact Loading," *Transactions of the SMiRT* 21, New Delhi, India.

Sugano T., Tsubota H., Kasai Y., Koshika N., Orui S., von Rieseman W.A., Bickel D.C. and Parks M.B. (1993). "Full-scale aircraft impact test for evaluation of impact force," *Nucl. Eng. and Design*, 140: 373-385.

Vepsä A. et al. (2011). "IRIS_2010 - Part II: Experimental Data," *Transactions of the SMiRT* 21, Div-V: Paper ID# 5206, New Delhi, India.

Vepsä, A., Lamula, L., Raunio, K. (2016). "IRIS 3 – Soft impact testing of a reinforced concrete structure," Research report VTT-R-04829-16, VTT.